Electrochemical Insertion of Hydrogen into Diniobium Pentaoxide

Teruhisa KOMURA,* Takahiro NAKANORI, and Koshin TAKAHASHI
Department of Materials Science and Engineering, Faculty of Technology, Kanazawa University, 2-40 Kodatsuno, Kanazawa 920

(Received May 10, 1993)

The electrical behavior of the Nb_2O_5 electrode in Na_2SO_4 solutions was characterized by the impedance spectra. The pH dependence of the flat band potential could be explained in terms of the acid-dissociating equilibrium of hydroxyl groups on the oxide surface. The plot of equilibrium potential of the oxide vs. pH gave a straight line with a slope of −0.06 V. The equilibrium potential became monotonously more negative with increasing extent of the reduction of the oxide. The cyclic voltammograms and chronopotentiograms of the partially reduced oxide indicated that the diffusion of an electroactive species in the oxide controlled the rate of the electrode process. These results suggest that $H_xNbO_{2.5}$ or $NbO_{2.5-x}(OH)_x$ can be formed by the reduction of the oxide. The conductivities of the oxide increased about two orders of magnitude by the insertion of a small amount of hydrogen. In conclusion, a blue coloration of the oxide can occur as a result of the diffusion of H^+ from the electrolyte into the Nb_2O_5 lattice and a simultaneous injection of electrons to d-block bands of Nb in the energy band model.

The transition metal oxides with tunnel networks or layered lattices can form nonstoichiometric hydrogen compounds by chemical reduction in acidic solutions.[1,2] The compounds are most aptly described as hydrogen insertion compounds since the parent oxide matrix is essentially unaltered. The insertion reactions have been extensively investigated in connection with their potential use in electrochromic display devices.[3,4] However, the slow dissolution of WO_3, MoO_3, and V_2O_5 in aqueous sulfuric acid solutions has prevented the application of these system to practical devices.

Reichman et al.[5] reported the preliminary experiments demonstrating electrochromic behavior of Nb_2O_5, which is insoluble in many media. The passive behavior[6] of the Nb_2O_5 film anodically grown on a Nb metal suggested that this oxide should be a promising material for electrochromic devices. In order to understand the phenomenon of the coloration of Nb_2O_5, it is necessary to have a detailed knowledge of the basic electrochemical properties of the oxide. In this paper, we describe a systematic investigation on the cathodic reduction of Nb_2O_5 electrodes.

Experimental

Diniobium pentaoxide electrodes were prepared by the oxidation of a Nb metal (99.95%) at 500 °C in air. The X-ray diffraction pattern of the oxide indicated that it was T-Nb_2O_5.[7] The amount of oxide was determined by weighing the sample before and after the thermal oxidation. The thickness (1—10 μm) of the oxide was estimated from a density[7] of 4.9 g cm^{-3} for the oxide. Sintered Nb_2O_5 electrodes were prepared by pressing powdered Nb_2O_5 (Kanto Chemicals, >99.95%) at 6 ton cm^{-2} and heating it at 800 °C in air for 16 h. All the chemicals were of GR grade and Na_2SO_4 was used after recrystallization. Electrolyte solutions were prepared with doubly-distilled water.

The conductivity of Nb_2O_5 was measured on a YHP 4261A or 4265B LCR meter at a frequency of 1 kHz in the temperature range 20—250 °C. Electrochemical experiments were carried out in a one-compartment, three-electrode glass cell at room temperature. A Ag|AgCl|KCl electrode and a large platinum gauze (>10 cm^2) were used as the reference and counter electrodes, respectively. Electrolytes were 0.5 M (M=mol dm^{-3}) Na_2SO_4 solutions whose pH's were adjusted with H_2SO_4. All solutions were purged with nitrogen gas prior to and during the electrochemical measurements. The impedance spectra of the Nb_2O_5electrode were obtained on a HP 4284A LCR meter over the frequency range from 20 to 10^6 Hz. The ac signal of 10 mV amplitude was applied between the working and counter electrodes. The differential capacitances of the oxide electrodes (area 0.075 cm^2) were measured at a frequency of 1 kHz. Partially reduced oxides were formed by the potentiostatic electrolysis of the Nb_2O_5 electrodes. The electric charge transferred during the reduction was counted on a Hokuto Denko HF-201 coulometer in the potential region with no evolution of a H_2 gas. The variation in conductivity of the oxide with the electrochemical reduction was measured by use of the sintered electrode, which had two gold films separated from each other by 0.1 mm on the back side of the electrode. After the sintered electrode was potentiostatically reduced, a dc voltage of 50 mV was applied between the two gold films. The flowing current was used to determine the resistance of the electrode at each electrode potential.

Results and Discussion

The measurement of the conductivity κ of Nb_2O_5 gave a linear relationship between $\log\kappa$ and the reciprocal of temperature T. The relationship was expressed by the following equation, with an error of about 0.05 in $\log\kappa$.

$$\log\frac{\kappa}{\mathrm{S\cdot cm^{-1}}} = -\frac{1810}{T/\mathrm{K}} - 1.82 \quad (290 \leqq T \leqq 520\ \mathrm{K}) \qquad (1)$$

The conductivity data indicated that the oxide was a semiconductor having a small conductivity (10^{-8} S cm^{-1}) at room temperature. Equation 1 gave a value of 0.36 eV for the activation energy of conduction. This value was fairly smaller than the bandgap energy (3.4

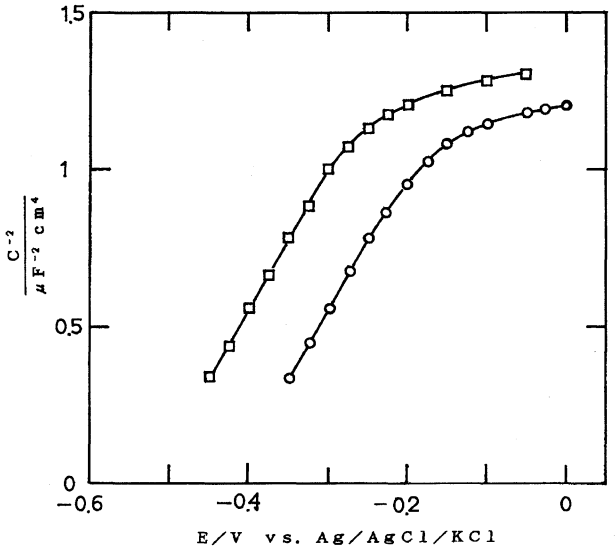

Fig. 1. Plots of reciprocal square of capacitance vs. electrode potential for Nb_2O_5 in 0.5 M Na_2SO_4 solutions. ○: pH 4.65, □: pH 6.50.

eV)[8] of Nb_2O_5. Since Nb_2O_5 is an oxygen-deficient oxide with reducible cation,[9] the observed activation energy probably corresponds to the ionization energy of oxygen vacancies which are donors.

Figure 1 shows the differential capacitances C of the Nb_2O_5 electrode in Na_2SO_4 solutions. The measured capacitance for a semiconductor electrodes can be equal to the capacitance of space charge region of the semiconductor, because the latter is generally much smaller than the capacitance (20—30 $\mu F\,cm^{-2}$) of the Helmholtz double layer at a solid-solution interface. In the absence of a high density of surface states, the capacitance C_{sc} of the space charge region is expected to vary with the electrode potential E according to the Mott–Schottky Eq. 2.[8]

$$\frac{1}{{C_{sc}}^2} = \frac{2}{\varepsilon_r \varepsilon_o e N A^2}(E - E_{fb} - kT/e), \qquad (2)$$

where E_{fb} is the flat band potential of a semiconductor, ε_r is its relative permittivity, N is the density of charge in the space charge region, and the other symbols have their usual meanings. We determined the flat band potential of the Nb_2O_5 electrode by extraporating the linear portion in the $1/C^2$ vs. E plots to $1/C^2=0$. The values of the flat band potential changed linearly with pH of the solution. A linear relationship between them was expressed by the following equation.

$$E_{fb} = -0.25 - 0.056\ \text{pH} \qquad (3)$$

At higher potentials than E_{fb}, the Faradiac charge transfer is negligible owing to the surface barrier on the oxide. The pH dependence of E_{fb} can be explained in terms of the acid-dissociating equilibrium of hydroxyl groups on the surface of the oxide (in other words, the adsorption–desorption of H^+ and OH^- on the oxide surface).

$$-OH_2^+ \underset{H^+}{\overset{-H^+}{\rightleftharpoons}} -OH \underset{H^+}{\overset{-H^+}{\rightleftharpoons}} -O^- \qquad (4)$$

An increase in pH causes the potential of the Helmholtz double layer to be lower because the oxide surface is more negatively charged. The point of zero charge (pzc) for the oxide with high oxidation number of metal ion is probably in low pH, for the pzc become more acidic with increasing charge/radius of a metal ion.[10] The experiment by Nechayev et al.[11] suggested that the pzc of Nb_2O_5 might be about pH 3. This pzc value gave a value of −0.42 V vs. Ag/AgCl/KCl to the flat band potential when the potential of the Helmholtz double layer was zero. We estimated the energy of conduction band edge at the pzc to be −0.78 V on the assumption that the Fermi level was equal to the donor level.

The slope of the linear $1/C^2$ vs. E plots can give the density of charge in the space charge region of the semiconductor. The charge density evaluated with a relative permittivity[6] of 46 was $(8\pm2)\times10^{17}$ cm^{-3} independently of pH. For Nb_2O_5 it is certainly the density of donors which probably are oxygen vacancies.

The $1/C^2$ vs. E plots showed a departure from the linearity at higher potentials. A possible explanation for the non-linearity of the plots might be a non-uniform distribution of defects in the oxide films. During the thermal oxidation of Nb, oxygen vacancies move between the metal-oxide and oxide-gas interfaces. Therefore, it seems reasonable to assume that the concentration gradient of defects exists in the oxide films.[12] Although the concentration profile of defects should be dependent on the film thickness, the variation of the donor density with the film thickness was not observed in a narrow range of thickness (1—10 μm).

Figure 2 shows the pH dependence of the equilibrium potential of Nb_2O_5 electrodes in Na_2SO_4 solutions. Curve 1 is for a pure oxide (colorless) and curve 2 for the partially reduced oxide (blue). For each oxide, the plot of the equilibrium potential vs. pH gave a straight line with a slope of −0.06 V. This result suggests that either the oxide surfaces may be more negatively charged with increasing pH or the oxide electrodes may electrochemically respond to H^+ in the solution. When the partially reduced oxide was exposed to air, the potential of the oxide moved slowly to the higher values with the simultaneous color change from blue to colorless. This indicates that the reduced oxide is oxidized by O_2, particularly in a sulfuric acid solution.

An increase in the extent of reduction of the oxide led to a lowering of the equilibrium potential of the oxide electrode. Figure 3 shows the relationship between the equilibrium potential and x which is the number of electrons transferred per mole of Nb during the ca-

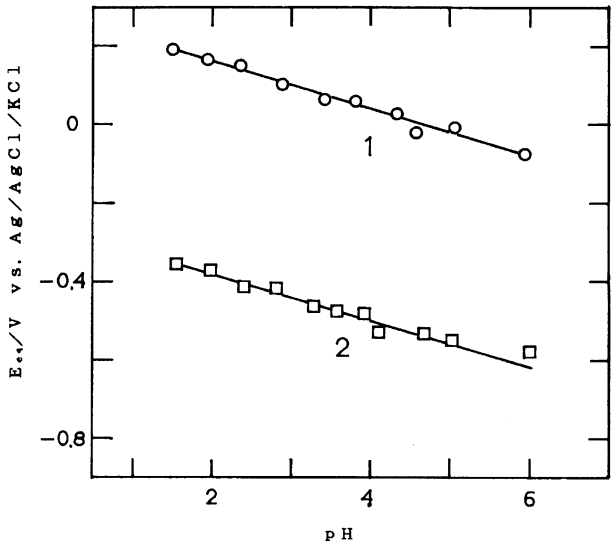

Fig. 2. The pH dependence of equilibrium potential of Nb_2O_5 electrode in Na_2SO_4 solutions. Curve 1: pure oxide, 2: partially reduced oxide.

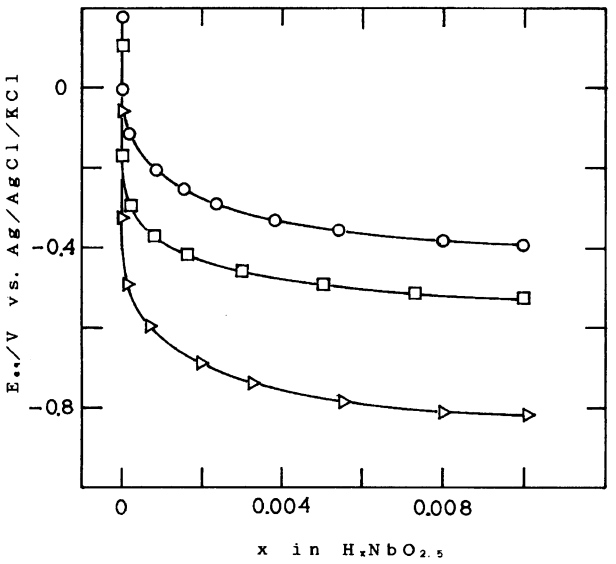

Fig. 3. Relationship between the extent of reduction of the oxide and equilibrium potential. ○: pH 0.80, □: pH 2.65, △: pH 5.30.

thodic reduction. In the shown range of x, no evolution of H_2 was observed in the cathodic reduction. The equilibrium potential became monotonously more negative with increasing x at each pH. The lowering of the equilibrium potential is probably due to an increase in the activity of an electroactive species in the oxide. Although the species could be indistinctly confirmed by the IR and X-ray studies, we regarded it as hydrogen on the basis of the following observations.

Figure 4 shows the cyclic voltammograms of the reduced oxide ($x=0.01$) at different scanning rates v of electrode potential. An anodic peak ascribable to the

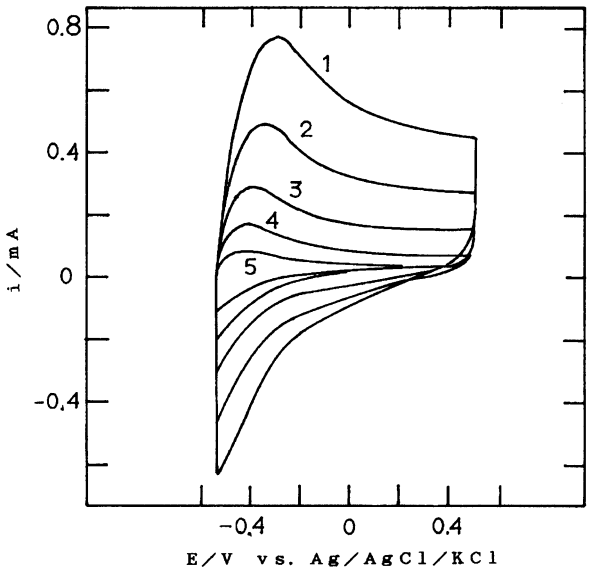

Fig. 4. Cyclic voltammograms of the reduced oxide ($x=0.01$) at different scanning rates of electrode potential. 1: 400, 2: 200, 3: 100, 4: 50, 5: 20 $mV\,s^{-1}$. pH 2.75.

oxidation of the electrode was observed. The linear dependence of the peak current on $v^{1/2}$ suggests that the current may be determined by the rate of diffusion process in the oxide. Anodic chronopotentiograms of the reduced oxide also showed the steep rise of electrode potential which was due to the reduction to zero of surface concentration of the electroactive species. The change of the transition time τ with current density is presented in Fig. 5 at different extents of reduction of the oxide. A linear $1/i-\tau^{1/2}$ relationship and an increase in τ with increasing x also indicate that the diffusion of the species in the oxide controls the rate of the electrode process.

The above results led to the conclusion that reaction 5 could occur on the Nb_2O_5 electrode.

$$H^+ + e \longrightarrow H \text{ in oxide.} \quad (5)$$

A blue coloration can result from the simultaneous injection of protons and electrons into the oxide. We express the reduced oxide as $H_xNbO_{2.5}$ or $NbO_{2.5-x}(OH)_x$ in the potential range with no evolution of a H_2 gas.

$$NbO_{2.5} + x(H^+ + e) \longrightarrow H_xNbO_{2.5} \quad (6)$$

$$NbO_{2.5} + x(H^+ + e) \longrightarrow NbO_{2.5-x}(OH)_x \quad (7)$$

The monotonous lowering of the equilibrium potential with increasing x implies no phase transition of the oxide in the range of $x<0.006$. Consequently, hydrogen may be topotactically inserted into the parent oxide matrix. Otherwise, we are able to have Eq. 8 as a alternative reaction.

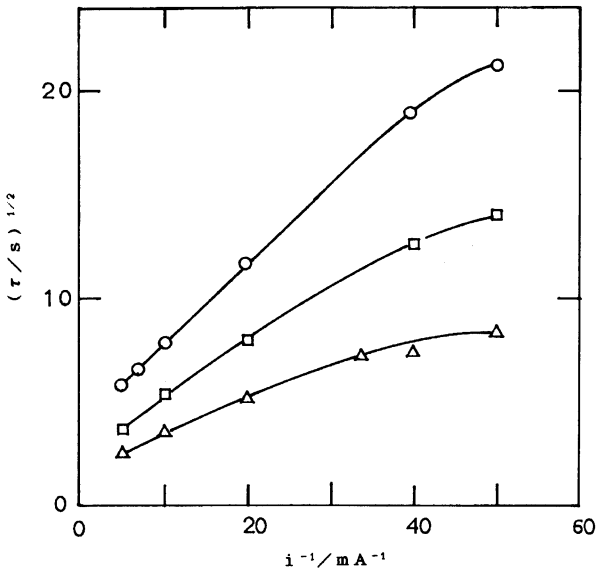

Fig. 5. Change of transition time in anodic chronopotentiometry of the reduced oxide with current density. ○: $x=5\times10^{-3}$, □: $x=2\times10^{-3}$, △: $x=5\times10^{-4}$.

$$NbO_{2.5} + x(H^+ + e) \longrightarrow NbO_{2.5-x/2} + x/2\ H_2O \quad (8)$$

The injected electrons are trapped in oxygen vacancies which are generated by the reaction of H^+ with the oxide surface. However, the magnitude of the measured diffusion coefficient denied the possibility of an increase in concentration of the lattice defects (see later).

Figures 6 and 7 show complex plane impedance and admittance plots, respectively, for the Nb_2O_5-solution interface. These diagrams suggested that the electrical characteristics of the interface could be represented by

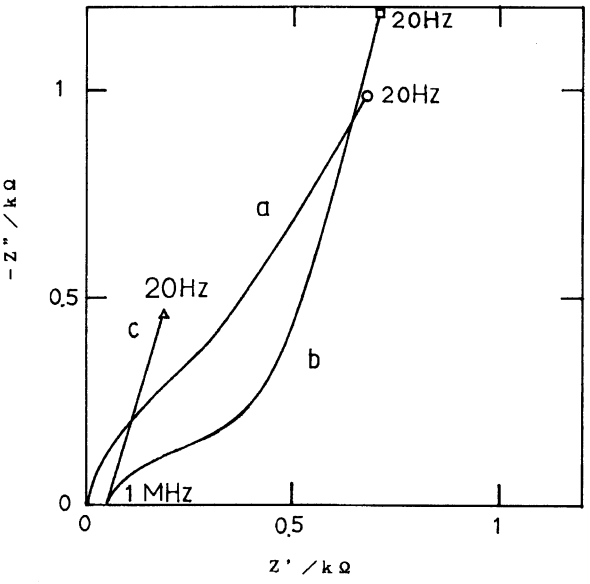

Fig. 6. Complex plane impedance plots for Nb_2O_5 electrode in Na_2SO_4 solution. Electrode potential; curve a (×1/10): 0, b: −0.2, c: −0.4 V.

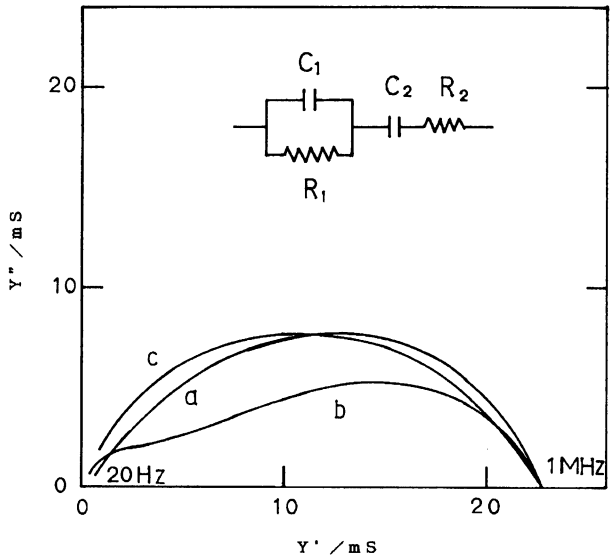

Fig. 7. Complex plane admittance plots. Electrode potential; curve a: 0, b: −0.2, c: −0.4 V.

the electric equivalent circuit in Fig. 7, although the impedance plots at lower frequencies wasn't perpendicular to the Z' axis owing to the leak in C_2. When the equivalent circuit is used, the point at which the impedance curve intersects with the Z' axis at higher frequencies gives a value of R_2. The points of intersection of the admittance curve with the Y' axis at higher frequencies and at lower frequencies give the values of $1/R_1+1/R_2$ and of $1/R_1$, respectively. Figure 6 indicates that R_2 is the resistance of the solution because its value (about 50 Ω) is independent of the electrode potential. Since $1/R_1 \ll 1/R_2$ in the examined range of the potential, an R_2 value of 43 Ω was also obtained from the admittance plots. At higher potentials than E_{fb}, the impedance curves had a semicircle corresponding to the portion of the R_1C_1 parallel circuit. The diameter of the semicircle decreased largely at more negative potentials. At lower potentials than E_{fb}, the electrical characteristics of the electrode could be preferably expressed by an RC series circuit. Therefore, R_1 and C_1 correspond to the resistance and capacitance of the oxide, respectively. It was difficult to determine a value of R_1 from the admittance curves because the plots at lower frequencies centered on the zero point in the diagram. Accordingly, the change in Z' values at 20 Hz with the insertion of hydrogen is shown in Fig. 8 (curve 1). The resistance of the oxide decreased about two orders of magnitude even at $x=0.006$. Curve 2 shows the change in resistance obtained by the dc method for the sintered electrode. The curve also indicates that the conductivities of the oxide increase about three orders of magnitude by the insertion of a small amount of hydrogen. Because Nb^{5+} has no valence electron, Nb_2O_5 is essentially an insulator in the absence of any defect in the oxide. The injected electrons probably occupied

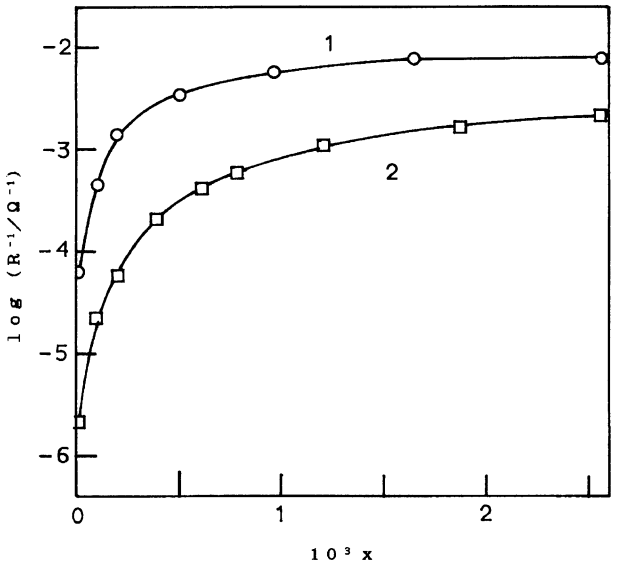

Fig. 8. Change in resistance of oxide electrode with insertion of hydrogen. Curve 1: Z' value at 20 Hz in impedance diagram, curve 2: resistance obtained by dc method for sintered electrode.

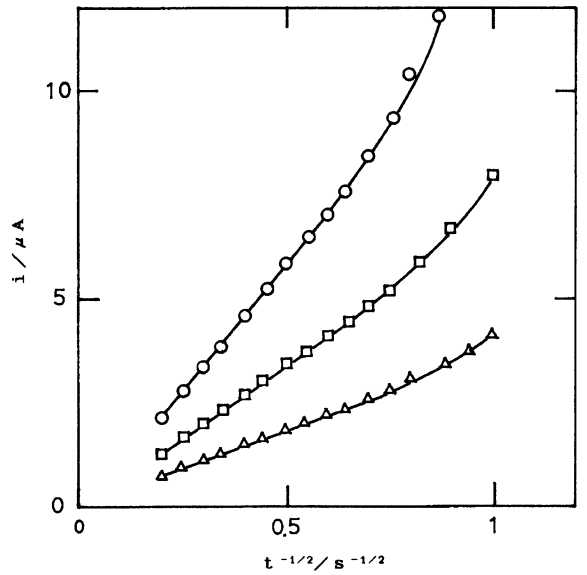

Fig. 9. Current–time curves after a potential step of 10 mV at different equilibrium potential. ○: −0.50, □: −0.45, △: −0.40 V.

d-block bands of Nb in the energy band model. Therefore, the inserted hydrogen could exist as proton in the oxide.

The mobility of hydrogen in Nb_2O_5 was evaluated by the potential step technique in which the transient current was controlled by the rate of the diffusion of hydrogen in the oxide. The theoretical treatment has been given by Wen et al.[13] Figure 9 shows the current–time curves after a potential step of 10 mV at different equilibrium potentials. The curves follow closely the Cottrell Eq. 9.

$$i = \frac{QD^{1/2}}{L(\pi t)^{1/2}} \qquad (t \ll L^2/D) \qquad (9)$$

where Q is the electric charge transferred after the potential step, D is the chemical diffusion coefficient of proton, and L is the thickness of the oxide film. The D values determined from the slope of the linear i vs. $t^{-1/2}$ plots are shown in Fig. 10. The values of D were about 10^{-10} $cm^2\,s^{-1}$. Although the conductivity of the oxide increased greatly by the insertion of a small amount of hydrogen, the D values were independent of x in the range of $x<0.008$. An ionic conductivity of 2×10^{-8} $S\,cm^{-1}$ at $x=0.002$ can be estimated from the measured value of D on the presumption that all the inserted hydrogens exist as protons. This result means that the increase in conductivity of the oxide is not due to an increase in ionic conduction. Because the diffusion coefficient of oxide ion is not more than 10^{-11} $cm^2\,s^{-1}$ even in ionic conductors such as $Ln_{1-x}Sr_xCoO_3$,[14] it may be much smaller in a common oxide. Therefore, the magnitude of the measured D values denied the possibility of reaction 8. A blue coloration can occur as a result of

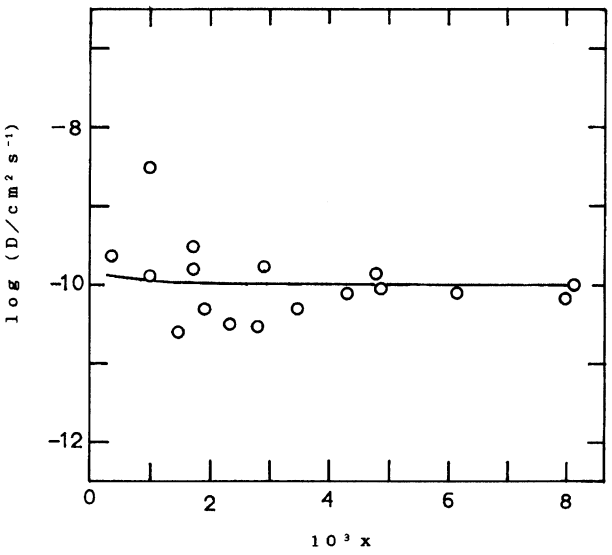

Fig. 10. Chemical diffusion coefficient of proton in Nb_2O_5.

the diffusion of H^+ from the electrolyte into the Nb_2O_5 lattice and a simultaneous injection of electrons from the metal-oxide interface.

Gomes et al.[15] reported that the D value was 10^{-7}—10^{-8} $cm^2\,s^{-1}$ and decreased appreciably with x. However, the D values in WO_3 were approximately in the range of 10^{-11} to 10^{-9} $cm^2\,s^{-1}$ although they varied fairly with a way of preparing the oxide.[16] There is a structural similarity between Nb_2O_5 and WO_3. Tungsten trioxide has a distorted ReO_3-type structure and Nb_2O_5 has the structure built from blocks of the ReO_3-type lattice.[17] Therefore, the mobility of proton in

Nb_2O_5 may be comparable to that in WO_3.

The dehydration of chemically reduced Nb_2O_5 powder resulted in rapid oxidation of the oxide by O_2. This fact suggests that water may play an important role in the coloration. As regards the chemical composition of the hydrogen insertion compound, we must await the further research.

References

1) R. Schollhorn, *Angew. Chem., Int. Ed. Engl.*, **19**, 983 (1980).

2) P. G. Dickens and M. F. Pye, in "Intercalation Chemistry," ed by M. Whittingham and A. Jacobson, Academic Press, New York (1982), p. 539.

3) A. D. Paola, F. D. Quarto, and C. Sunseri, *J. Electrochem. Soc.*, **125**, 1344 (1978).

4) B. Reichman and A. J. Bard, *J. Electrochem. Soc.*, **126**, 583 (1979).

5) B. Reichman and A. J. Bard, *J. Electrochem. Soc.*, **127**, 241 (1980).

6) S. Hornkjol, *Electrochim. Acta*, **36**, 1443 (1991).

7) H. Schafer, R. Gruehn, and F. Schulte, *Angew. Chem., Int. Ed. Engl.*, **5**, 40 (1966).

8) S. R. Morrison, "Electrochemistry at Semiconductor and Oxidized Metal Electrodes," Plenum Press, New York (1980), p. 119.

9) K. E. Heusler and M. Schulze, *Electrochim. Acta*, **20**, 237 (1975).

10) G. A. Parks, *Chem. Rev.*, **65**, 177 (1965).

11) Y. A. Nechayev and V. N. Sheyin, *Kolloidn. Zh.*, **41**, 361 (1979).

12) F. D. Quarto, A. D. Paola, and C. Sunseri, *Electrochim. Acta*, **26**, 1177 (1981).

13) C. J. Wen, B. A. Boukamp, and R. A. Huggins, *J. Electrochem. Soc.*, **126**, 2258 (1979).

14) T. Kudo, H. Obayashi, and T. Gejo, *J. Electrochem. Soc.*, **122**, 159 (1975).

15) M. A. Gomes and L. O. S. Bulhoes, *Electrochim. Acta*, **34**, 765 (1989).

16) H. L. Hitchmann, *Thin Solid Films*, **61**, 341 (1979); J. P. Randin and R. Viennet, *J. Electrochem. Soc.*, **129**, 2349 (1982).

17) A. F. Wells, "Structural Inorganic Chemistry," Clarendon Press, Oxford (1975), p. 439.